CHEMISTRY
A European Journal

www.chemeurj.org

Reprint

A Journal of
ChemPubSoc Europe
ACES
Asian Chemical Editorial Society
WILEY-VCH

ChemPubSoc Europe

DOI: 10.1002/chem.201905075

CHEMISTRY A European Journal Full Paper

Drug Delivery

Insulin Delivery from Glucose-Responsive, Self-Assembled, Polyamine Nanoparticles: Smart "Sense-and-Treat" Nanocarriers Made Easy

Maximiliano L. Agazzi,[a] Santiago E. Herrera,[a] M. Lorena Cortez,[a] Waldemar A. Marmisollé,[a] Mario Tagliazucchi,[b] and Omar Azzaroni*[a]

Abstract: Polyamine–salt aggregates (PSA) are biomimetic soft materials that have attracted great attention due to their straightforward fabrication methods, high drug-loading efficiencies, and attractive properties for pH-triggered release. Herein, a simple and fast multicomponent self-assembly process was used to construct cross-linked poly(allylamine hydrochloride)/phosphate PSAs (hydrodynamic diameter of 360 nm) containing glucose oxidase enzyme, as a glucose-responsive element, and human recombinant insulin, as a therapeutic agent for the treatment of diabetes mellitus (GI-PSA). The addition of increasing glucose concentrations promotes the release of insulin due to the disassembly of the GI-PSAs triggered by the catalytic in situ formation of gluconic acid. Under normoglycemia, the GI-PSA integrity remained intact for at least 24 h, whereas hyperglycemic conditions resulted in 100% cargo release after 4 h of glucose addition. This entirely supramolecular strategy presents great potential for the construction of smart glucose-responsive delivery nanocarriers.

Introduction

Rational and nature-inspired engineering of responsive delivery nanoarchitectures has emerged as a fascinating challenge in materials science and modern biomedicine.[1–6] Within this context, the development of intelligent glucose-sensitive delivery devices to treat diabetes mellitus has prompted substantial research advances.[7–10] This metabolic disease is characterized by a deficit of endogenously produced insulin (Ins) and/or Ins resistance that leads to elevated blood glucose levels (hyperglycemia).[11] Currently, diabetes mellitus affects more than 400 million people around the world, and thus, is one of the most serious threats to global public health.[12,13] In general, diabetic patients self-administer Ins with multiple subcutaneous injections to control blood glucose levels.[14–16] However, this methodology is usually painful and requires strict compliance on the part of the patient. In addition, open-loop subcutaneous administration of Ins often regulates the glucose levels inadequately, causing very severe disorders.[17–19] Therefore, several investigations have focused on the design of glucose-sensitive delivery systems with the capacity to sense glucose levels and use this information to selectively activate Ins release under hyperglycemia conditions (closed-loop Ins delivery).[18,20–22] Generally, to achieve a selective response, a glucose-responsive material is incorporated into the delivery platform, such as the glucose oxidase enzyme (GOx).[23,24] GOx catalyzes the oxidation of D-glucose to gluconic acid, which, in turn, reduces the local pH.[25–27] In this way, acidic pH can lead to conformational or structural changes in the delivery systems that ultimately drive the release of Ins.

Glucose-sensitive materials with entrapped GOx have been increasingly studied by employing architectures based on hydrogels, microgels, and multilayer films,[28–30] in which GOx is immobilized in complex macromolecular systems.[31] The use of tailorable polymeric (nano)particles offers attractive features for drug-delivery systems, including suitable colloidal stability, large surface to volume ratios, high loading capacity, long circulation time in plasma, and ability to cross biological membranes.[32–36] In this way, several self-regulated Ins-delivery systems based on vesicles, micelles, and nanogels have been presented.[37–42] Typically, these nanocarriers are formed by self-assembly or cross-linking of sensitive block copolymers. The synthesis of these building blocks requires multistep processes that increase costs and hinder the design scalability for practical applications. Therefore, the development of facile and robust engineering approaches to build innovative nanoscale platforms is an exciting challenge.

[a] Dr. M. L. Agazzi, Dr. S. E. Herrera, Dr. M. L. Cortez, Prof. Dr. W. A. Marmisollé, Prof. Dr. O. Azzaroni
Instituto de Investigaciones Fisicoquímicas Teóricas y Aplicadas Facultad de Ciencias Exactas, Universidad Nacional de La Plata-CONICET Sucursal, 4, Casilla de Correo 16, 1900 La Plata (Argentina)
E-mail: azzaroni@inifta.unlp.edu.ar

[b] Prof. Dr. M. Tagliazucchi
Departamento de Química Inorgánica, Analítica y Química Física INQUIMAE-CONICET, Facultad de Ciencias Exactas y Naturales
Ciudad Universitaria, Pabellón 2, Buenos Aires C1428EHA (Argentina)

Supporting information and the ORCID identification number(s) for the author(s) of this article can be found under: https://doi.org/10.1002/chem.201905075.

In parallel, bioinspired polyamine–salt aggregates (PSA), based on the ionic cross-linking of polyamines, have been intensively explored in recent decades for the delivery of drugs, proteins, genes, and medical imaging agents.[43,44] These soft materials have become a focus of attention, mainly due to three crucial advantages: 1) their preparation involves a very simple, one-step process based on a mixture of dilute polyelectrolyte solutions with multivalent salts under mild conditions;[45,46] 2) their three-dimensional matrices present a great capacity to integrate different types of bioactive and functional compounds;[47–52] and 3) they respond to external stimuli, such as pH and ionic strength, because the supramolecular network is essentially stabilized by electrostatic interactions.[53–56] Within this framework, poly(allylamine hydrochloride) (PAH) was used as a building block to generate PSA by cross-linking with simple inorganic phosphate (Pi).[57,58]

In this sense, PAH/Pi PSA has been used to encapsulate functional compounds, such as indocyanine green (ICG) and curcumin.[59–61] Moya and co-workers also used PAH/Pi PSA as a nanocarrier for the pH-triggered release of small interfering RNA (siRNA).[62] They found that PSA loaded with siRNA remained stable at physiological pH, and released its cargo in acidic endosomes, where protonation of the phosphate groups destabilized the electrostatic interactions that supported the ionically cross-linked matrix. Recently, we explored the physicochemical properties and the pH/ionic strength response of PAH/Pi PSA in the solution phase.[63] We also used PSAs loaded with a model molecular dye as building blocks for the construction of multilayer films with attractive properties for pH-controlled release.[64]

Herein, we show, for the first time, the coimmobilization and rational integration of proteins in cross-linked PAH/Pi PSA. In particular, we pursue the goal of integrating both GOx and Ins into the ionically cross-linked PAH/Pi matrix to obtain a new kind of glucose-responsive soft material. We demonstrate that it is possible to generate the multicomponent nanoarchitecture by a simple preparation process and that the resulting supramolecular nanocarriers present interesting properties for glucose-regulated Ins delivery.

Experimental Section

Chemicals

PAH (MW≈17 500), GOx from *Aspergillus niger* (type VII), human recombinant Ins (SAFC, 91077C), and 4-(2-hydroxyethyl)piperazine-1-ethanesulfonic acid (HEPES) were purchased from Sigma Aldrich. Sodium phosphate monobasic monohydrate (Pi) was purchased from Cicarelli. D-(+)-Glucose (Glu), sodium hydroxide, and hydrochloric acid were purchased from Anedra. All chemicals were used without further purification.

GOx–Ins-containing PSA (GI-PSA) assembly

To obtain a GI-PSA colloidal dispersion (10 mL), we consecutively mixed the following solutions in a 50 mL beaker under constant stirring (50 rpm): 1) PAH (2.34 mL, 20 mM, monomer concentration), 2) HEPES buffer (22.1 mL, 20 mM, pH 7.4), 3) GOx (1.95 mL, 2 mg mL^{-1}), 4) Ins (1.95 mL, 2 mg mL^{-1}), and 5) Pi (1.731 mL, 10 mM). All solutions (PAH, GOx, Ins, and Pi) were freshly prepared by using a 20 mM aqueous solution of HEPES buffer as solvent and their pH values were adjusted to 7.4 by using 1 M HCl or 1 M NaOH prior to mixing. We added each solution very quickly to the beaker to avoid heterogeneous reactions and waited 5 min between the addition steps. After the incorporation of Pi, a cloudy solution (30 mL) was obtained (0.13 mg mL^{-1} Ins, 0.13 mg mL^{-1} GOx, 1.56 mM PAH, and 0.577 mM Pi). The as-prepared colloidal dispersion was allowed to stabilize for 2 h under stirring to complete the cross-linking process. The dispersion was then centrifuged at 4000 rpm (1310 *g*) for 30 min and the supernatant was discarded to remove excess reactants (UV/Vis analysis of the polypeptide content in the supernatant is shown in Figure S1 in the Supporting Information). The precipitate was concentrated three times in 20 mM HEPES buffer (pH 7.4) and resuspended by ultrasonication for 15 min to yield the GI-PSA colloidal dispersion (10 mL). The resuspended dispersion was used for pH- and glucose-triggered disassembly experiments.

GI-PSA disassembly by external pH changes

The turbidity of the GI-PSA colloidal dispersion was tested at different pH values by measuring the transmittance percentage (%T) at $\lambda = 580$ nm (light-scattering effects). To study the disassembly process, 50 mM HCl was added in small aliquots (0.5–2 μL) to GI-PSA colloidal dispersion (2 mL), while measuring pH and %T. A clear solution (100 %T) indicated total GI-PSA disassembly.

GI-PSA disassembly by glucose addition

For glucose-induced disassembly studies, GI-PSA colloidal dispersion (2 mL) was placed in a plastic cuvette and thermostated at 37 °C. A small volume of 0.5 M glucose in 20 mM HEPES buffer (pH 7.4) was added to the cuvette and the chronometer was turned on. The solution was gently air-injected every 20 min and both the pH and %T at $\lambda = 580$ nm were registered, keeping the temperature stable at 37 °C. The pH values were recorded by using a capillary pH electrode connected to an ADWA AD8000 pH meter.

Dynamic light scattering (DLS) measurements

DLS measurements were carried out by using a ZetaSizer Nano (ZEN3600, Malvern, UK) at 37 °C by employing DTS1060 disposable cuvettes. The detector was placed at 173° backscatter angle and all measurements were conducted on 10 runs of 20 s.

TEM measurements

TEM images were obtained by using a JEOL microscope (120 kV) equipped with a Gatan US1000 charge-coupled device (CCD) camera. Samples were stained with phosphotungstic acid and adsorbed on carbon grids. The GI-PSA transference to the grids was achieved by forming a meniscus between the grid (top) and a concentrated GI-PSA colloidal dispersion (bottom) for a few seconds, followed by air-drying.

Circular dichroism (CD) spectroscopy measurements

CD measurements were performed by using a Jasco (Tokyo, Japan) J-815 CD spectrometer at 20 °C. A quartz cuvette with a 1 mm path length was used for the peptide region ($\lambda = 200$–250 nm). Each spectrum was the result of averaging five consecutive scans. PSA sample contained GOx (0.13 mg mL^{-1}), PAH (1.56 mM), and Pi

(0.577 mM) in 20 mM HEPES buffer at pH 7.4. Free GOx sample contained GOx (0.13 mg mL^{-1}) in 20 mM HEPES buffer at pH 7.4.

Transmittance (%T) measurements

The transmittance of GI-PSA colloidal dispersions was measured by using an Ocean Optics DH-2000 instrument at $\lambda = 580$ nm with 1 cm light-path plastic cuvettes.

UV/Vis spectroscopy measurements

UV/Vis experiments were carried out by using a PerkinElmer Lambda 35 spectrometer and a 2 mm light-path quartz cuvette.

Results and Discussion

GI-PSA characterization and pH-triggered disassembly

By a simple combination of the individual building blocks under mild conditions (room temperature, neutral pH, atmospheric pressure, and aqueous solution), we constructed GI-PSA (Scheme 1). At pH 7.4, the negative net charge of these two proteins allows for their integration into the GI-PSA cross-linked structure. As we previously showed, the main phosphate species that contributed to the PAH/Pi PSA assembly was the HPO_4^{2-} anion, which strongly interacted with the positively charged amine groups in PAH chains.[63]

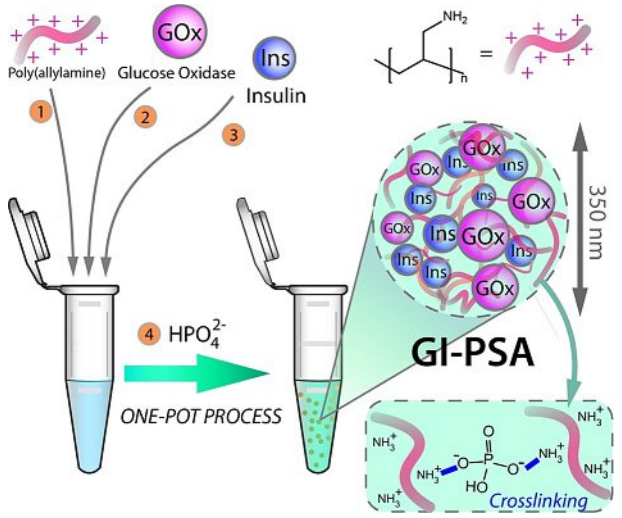

Scheme 1. GI-PSA formation at neutral pH. PAH cross-linking with phosphate anions and coencapsulation of GOx (violet spheres) and Ins (blue spheres).

Figure 1a shows the size distribution of GI-PSAs obtained from DLS measurements at 37 °C (pH 7.4). A single peak centered at 360 nm, with a polydispersity index of 0.1, indicates a narrow and homogeneous distribution of sizes in the solution phase. This result is consistent with the hypothesis that the cross-linking of PAH occurs concomitantly with the uptake of Ins and GOx. On the other hand, the TEM image in Figure 1b shows that GI-PSAs have a spherical shape and a wide distribution of particle diameters, with a maximum at 90 nm and a tail at larger diameter. The fact that TEM sizes are smaller than

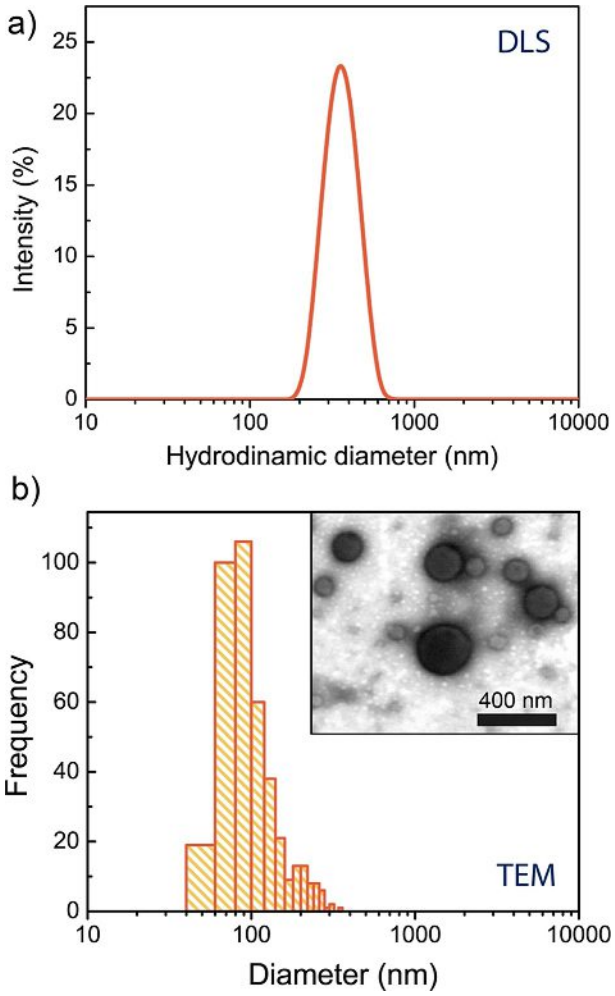

Figure 1. GI-PSA size distribution obtained by DLS (a) and TEM (b) analyses. Inset shows a TEM image of a GI-PSA sample.

those observed by DLS is probably due to dehydration of the sample for TEM measurements. Furthermore, GI-PSAs may suffer partial deformation upon contact with surfaces.[64]

We tested the stability of GI-PSAs over time to evaluate the possibility of nonselective undesired release of proteins. For this purpose, after 24 h of assembly, the sample was centrifuged, and the supernatant was analyzed by means of UV/Vis spectroscopy. Both GOx and Ins have absorption bands at around 275 nm due to the presence of tryptophan or tyrosine residues.[65,66] In addition, GOx exhibits absorption bands at $\lambda =$ 375 and 450 nm that are characteristic of the flavin adenine dinucleotide cofactor bound to the protein structure.[67] The spectrum of the supernatant showed a much smaller absorption in the UV and visible regions than that of a solution containing only GOx and Ins at the same final concentration of the colloidal sample (0.39 mg mL^{-1}). This result indicates that the protein cargo is efficiently encapsulated inside the GI-PSA structure and stabilized by supramolecular interactions and that undesired protein release does not occurs (Figure S2 in the Supporting Information). This result is not trivial because it shows that it is possible to rationally integrate two functional

proteins in PAH/Pi PSAs through a simple protocol and by using only supramolecular interactions. Previously, Anderson and co-workers reported the development of glucose-responsive microgels based on a physically cross-linked matrix of chitosan/tripolyphosphate loaded with Ins.[28] However, in that example, the GOx enzyme had to be first covalently encapsulated in nanocapsules and then incorporated into the microgels.

The secondary structure of GOx encapsulated in PSA was studied by means of CD spectroscopy. Figure S3 in the Supporting Information shows the far-UV CD spectra of free and encapsulated GOx in HEPES buffer at pH 7.4. The CD spectrum of native GOx exhibited two negative minima in the ultraviolet region at around 207 and 220 nm, which are characteristic of an α-helical conformation.[68–71] GOx within PSA also presents a negative shift in the CD signal, similar to that observed for the free enzyme, revealing a permanence of the helix conformation. However, the CD band at 207 nm is lowered its intensity to 60%. This could indicate a decrease in the α-helical content and changes in the secondary structure of the enzyme due interactions with polyamine chains.

As we previously reported, a PAH/Pi cross-linked colloid can be disassembled by altering the pH of the solution.[63] At low ionic strength conditions, if the pH is below 5.5, the HPO_4^{2-} anions that act as a GI-PSA cross-linker get protonated completely to form the $H_2PO_4^{1-}$ ions. Because this monovalent anion is not able to act as a cross-linking agent, the complete dissolution of GI-PSAs results. On the other hand, if the pH is raised above 9.7, the amine groups in PAH are deprotonated and GI-PSAs also dissolve. This behavior represents one of the key features of GI-PSAs that can be used for pH-triggered release of therapeutic drugs.[43,44,72]

The integrity of GI-PSAs was evaluated as a function of pH by measuring the light scattering of a colloidal dispersion of GI-PSA at different pH values. For this purpose, we measured the transmittance of the sample at $\lambda = 580$ nm, while lowering the pH by adding small aliquots of HCl. Light extinction at this wavelength is exclusively due to scattering; therefore, an increase in the transmittance reflects a decrease of either the number of or mean size of GI-PSA particles. Figure 2a shows the transmittance at $\lambda = 580$ nm between pH 7.4 and 4. A slow increase in the transmittance is detected until pH 5.25 and, after this point, a marked increase is observed, reaching 50% transmittance at pH 5.1 and 100% at pH 4.8. Figure 2b shows two photographs of the sample before and after disassembly. In the latter, a translucent solution indicates quantitative dissolution of GI-PSA colloids upon the addition of acid. The critical pH required to dissolve the colloids is lower in the present system than that in an analogous system without Ins and GOx.[63] This extra stabilization produced by the addition of proteins can be attributed to electrostatic coupling between the negatively charged Ins/GOx macromolecules ($pI_{Ins} = 5.3$; $pI_{GOx} = 4.2$) and the protonated PAH chains.[65,73,74] In other words, the proteins also act as cross-linking agents together with the phosphate anions.

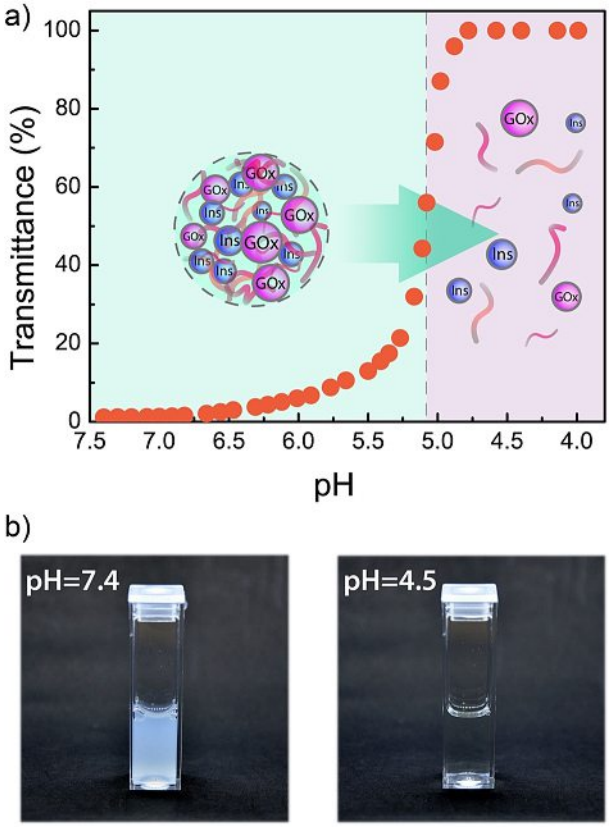

Figure 2. a) Total transmittance at $\lambda = 580$ nm for a colloidal dispersion of GI-PSA versus pH. The pH was externally adjusted by the addition of HCl. b) Photographs of the colloidal dispersion of GI-PSA at pH 7.4 (left) and 4.75 (right).

Glucose-triggered GI-PSA disassembly

GOx enzyme catalyzes the oxidation of glucose by dissolved molecular oxygen.[25,75] The products of the reaction are D-glucono-δ-lactone and hydrogen peroxide. In a subsequent reaction step, D-glucono-δ-lactone hydrolyzes to gluconic acid ($pK_a = 3.86$). Thus, at pH values higher than that of the pK_a of gluconic acid, the oxidation of glucose concomitantly releases protons that lower the pH of the solution. In this way, the oxidation of glucose catalyzed by GOx loaded into the GI-PSA is expected to dissolve the colloids by indirect shifting of the solution pH.

To evaluate the glucose responsiveness, GI-PSAs were incubated at 37 °C in solutions with different glucose concentrations, including hyperglycemic levels (10, 15, and 20 mM),[76] a normoglycemic level of 5 mM,[77] and a control level of 0 mM. We recorded the time variation of pH and %T immediately after the addition of glucose (see Figure 3a and b, respectively). The results show that the pH drops over time and the rate of pH change increases with increasing glucose level. This behavior reveals that GOx, immobilized in the ionic matrix, preserves its catalytic capabilities. On the other hand, under conditions of normoglycemia (5 mM), the pH reaches a constant value of 6.75 after 4 h, and then it remains stable for more than 2 days (not shown).

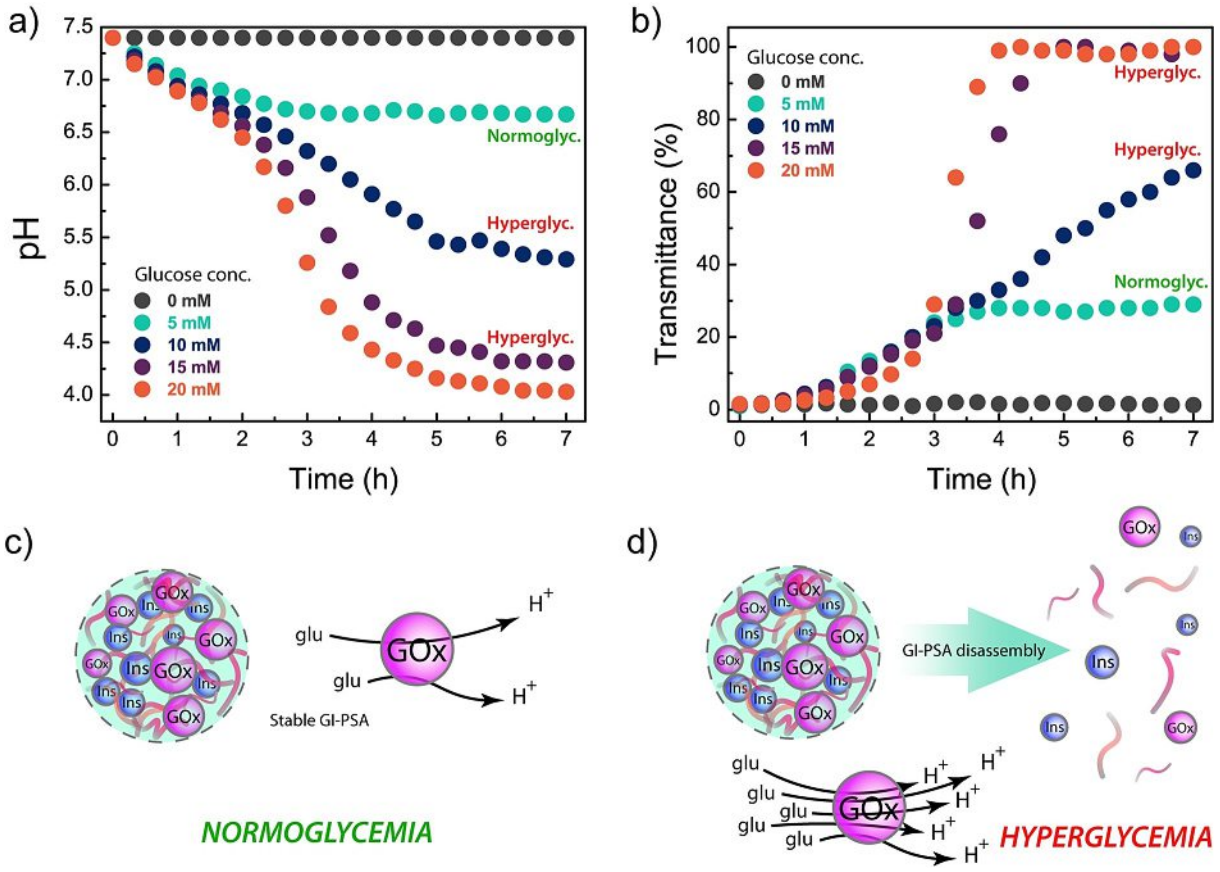

Figure 3. Time evolution of GI-PSAs after the addition of 0, 5, 10, 15, and 20 mM glucose: a) pH versus time and b) transmittance at $\lambda = 580$ nm versus time. Simplified representation of GI-PSA stability in normoglycemia (c) and hyperglycemia (d).

The time variation of the sample transmittance (Figure 3b) shows a marked increase for 20 and 15 mM glucose concentration, reaching $\%T = 100\%$ after 4 and 5 h, respectively. This result indicates that the total dissolution of GI-PSAs is achieved under hyperglycemic conditions (Figure 3d), which releases the total content of protein into the media. The complex evolution of pH over time observed in Figure 3a can be numerically simulated by considering the acid/base equilibria of different components in solution and typical Michaelis–Menten kinetics of the enzyme. Figure S4 in the Supporting Information shows that both experimental and theoretical curves follows the same sigmoidal shape, and thus, demonstrates that the changes in pH of the solution can be explained in terms of a combination between the rate of gluconic acid production by GOx and the different degrees of acid and buffer dissociation. A detailed description of the model used to calculate the pH changes over time is presented in the Supporting Information. For both 15 and 20 mM samples, total GI-PSA disassembly is achieved if the pH reaches a critical value of 4.5 (Figure 3a), similar to the dissolution pH obtained in the pH-forced disassembly experiment (Figure 2a). This result is consistent with the hypothesis that the dissolution of GI-PSAs is produced by the partial protonation of HPO_4^{2-} and the consequent loss of its cross-linking properties. This result has great significance because it proves that the release of Ins can be indirectly triggered by increasing glucose concentration.

In the case of 10 mM glucose concentration, a constant increase in transmittance is detected during 7 h, whereas under conditions of normoglycemia (5 mM) the transmittance linearly increases for the first 3.5 h and finally reaches a stable value of 26% that remains constant over 2 days at 37 °C (not shown). After this period of time, the sample (5 mM) was analyzed by DLS to obtain a homogeneous distribution of particle sizes, with a maximum centered at a diameter of 400 nm (Figure S5b in the Supporting Information), similar to that of a freshly prepared colloidal suspension of GI-PSA (Figure 1a). This observation indicates that, if the pH is high enough (pH 6.75), GI-PSAs remain stable in solution due to the presence of HPO_4^{2-} anions acting as cross-linking agents (Figure 3c).

Figure 4 shows the GI-PSA response time (defined as the time at which the colloidal suspension reaches 50% transmittance at $\lambda = 580$ nm) as a function of the concentration of added glucose. The obtained data indicate that the disassembly kinetics of GI-PSAs can be easily modulated by changing the glucose concentration. Also, the GI-PSA disassembly time decreases considerably as the glucose concentration increases, until reaching a constant value at around 1.5 h for glucose levels higher than 30 mM. The Michaelis constant for GOx with glucose is around 20 mM,[75] which indicates that the appearance of the plateau in Figure 4 is probably caused by the saturation of the enzyme at high glucose concentration.

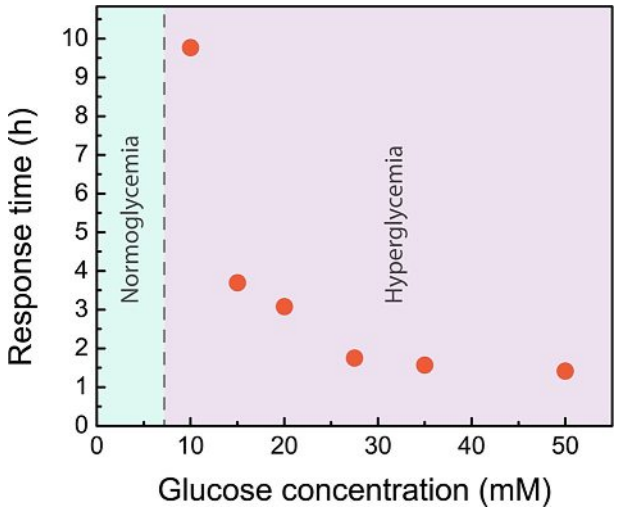

Figure 4. GI-PSA response time (%T ($\lambda = 580$ nm) = 50%) versus glucose concentration. GOx saturation effects.

Finally, we evaluated the glucose-triggered Ins release. The percentage of total protein (GOx + Ins) released was measured after 48 h of GI-PSA incubation with different concentrations of glucose (Figure 5). For this purpose, each colloidal suspension of GI-PSA was centrifuged, and the corresponding supernatants were analyzed by means of UV/Vis spectroscopy (Figure 5a). The total protein content, referred to as 100%, was obtained by analyzing the UV/Vis spectrum at $\lambda = 275$ nm of a solution of GI-PSA after complete disassembly with HCl (pH 4.5).

Figure 5b shows that, in the absence of glucose, the release of proteins from GI-PSAs is 9%. This small value indicates that the system has a suitable stability and keeps its cargo trapped after 48 h of preparation. Under normoglycemia conditions (5 mM of glucose), a small release of around 15% of the total trapped protein was found, which was in congruence with the minor changes of pH and transmittance as a function of time observed in Figure 3. In addition, this observation is in line with the homogeneous distribution of particle sizes found by means of DLS after 48 h of incubation (Figure S5 in the Supporting Information). If the GI-PSAs were exposed to hyperglycemia conditions, the amount of released protein grew considerably, reaching 100% for 15 and 20 mM glucose, in accordance with the complete GI-PSA disassembly observed in Figure 3. If 10 mM glucose was added, 40% of the total polypeptide was released, which indicated that 60% remained linked to the GI-PSA structure after 48 h. The change in the amount of released protein with glucose concentration indicates that our nanocarrier has the ability to self-regulate the Ins release rate and fraction, depending on the concentration of glucose in the media.

Conclusion

A new Ins-delivery approach has been proposed based on the coimmobilization of GOx and Ins in a biomimetic PSA. This straightforward engineering route leads to the successful construction of entirely supramolecular spherical nanocarriers by simple mixing the subunits under mild conditions.

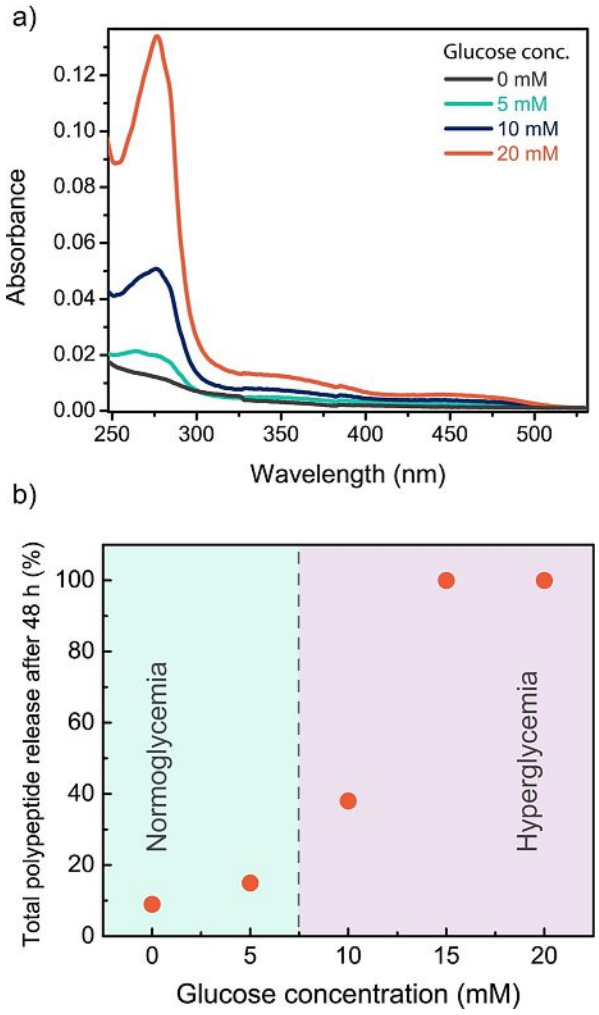

Figure 5. a) UV/Vis spectra of centrifuged GI-PSA supernatant 48 h after glucose addition, and b) percentage of total protein released (GOx + Ins) into the solution by spectral analysis at $\lambda = 275$ nm.

The GI-PSA obtained in this work has the capacity to sense glucose levels and respond by activating the release of Ins. Under hyperglycemic conditions, GOx trapped in the GI-PSA colloids converted glucose into gluconic acid, which resulted in an acidic environment that triggered the dissociation of ionic pairs in the supramolecular structure and, consequently, promoted the release of Ins. In contrast, negligible Ins release was observed under normoglycemia conditions.

We believe this PSA-based noncovalent strategy has great potential for the generation of an efficient and robust glucose-responsive, Ins-delivery system. To adjust the system to operate under physiological conditions, further studies must be carried out by checking the GI-PSA stability over time under in vivo conditions for different glucose levels and GOx contents. The main challenge in the application of glucose-responsive systems is to achieve a rapid response rate in a physiological environment with highly regulated pH. In this sense, it is essential that the glucose responsiveness under hyperglycemia

conditions generates a fast change of local pH that overcomes the physiological regulation and activates the selective release of Ins. Although direct comparison with other GOx-based platforms is difficult due to the different experimental conditions used in each case, under in vitro conditions other pH-controlled Ins release systems exhibit responses on timescales similar to that observed for our system.[30,40] Interestingly, some of these systems were explored in vivo by subcutaneous administration in 3D-gel-based configurations and showed great ability to regulate blood glucose concentrations.[28,37] Thus, a future challenge for the implementation of PSA as an effective on-demand Ins-releasing agent could be the development of semipermeable PSA shells that allow significant local pH changes despite the natural pH regulation of the body.

Finally, it is worth highlighting that the successful coimmobilization of two biomacromolecules, such as GOx and Ins, opens up the possibility of exploring the encapsulation and hierarchical combination of other therapeutic and functional agents into polyamine/phosphate PSAs, as well as the possibility of developing nanoreactors for enzymatic cascade reactions.

Acknowledgements

This work was supported by the Consejo Nacional de Investigaciones Científicas y Técnicas (CONICET, Argentina; grant no. PIP 0370), the Agencia Nacional de Promoción Científica y Tecnológica (ANPCyT, Argentina; PICT-2016-1680, PICT-2017-1523), the Austrian Institute of Technology GmbH (AIT-CONICET Partner Group: "Exploratory Research for Advanced Technologies in Supramolecular Materials Science", Exp. 4947/11, Res. No. 3911, 28-12-2011), and the Universidad Nacional de La Plata (UNLP). M.L.C., W.A.M, M.T., and O.A. are staff members of CONICET. M.L.A and S.E.H. gratefully acknowledge CONICET for their postdoctoral fellowships. We gratefully acknowledge Dr. Pablo H. Di Chenna for his helpful assistance during CD measurements.

Conflict of interest

The authors declare no conflict of interest.

Keywords: drug delivery · molecular recognition · nanostructures · self-assembly · supramolecular chemistry

[1] B. Taghizadeh, S. Taranejoo, S. A. Monemian, Z. Salehi Moghaddam, K. Daliri, H. Derakhshankhah, Z. Derakhshani, *Drug Delivery* **2015**, *22*, 145 – 155.
[2] M. Karimi, A. Ghasemi, P. Sahandi Zangabad, R. Rahighi, S. M. Moosavi Basri, H. Mirshekari, M. Amiri, Z. Shafaei Pishabad, A. Aslani, M. Bozorgomid, D. Ghosh, A. Beyzavi, A. Vaseghi, A. R. Aref, L. Haghani, S. Bahrami, M. R. Hamblin, *Chem. Soc. Rev.* **2016**, *45*, 1457 – 1501.
[3] M. Liu, H. Du, W. Zhang, G. Zhai, *Mater. Sci. Eng. C* **2017**, *71*, 1267 – 1280.
[4] L. Zhao, Q. Zou, X. Yan, *Bull. Chem. Soc. Jpn.* **2019**, *92*, 70 – 79.
[5] K. Ariga, D. T. Leong, T. Mori, *Adv. Funct. Mater.* **2018**, *28*, 1702905.
[6] M.-T. Li, M. Liu, Y.-H. Yu, A.-W. Li, H.-B. Sun, *Bull. Chem. Soc. Jpn.* **2019**, *92*, 283 – 289.
[7] R. Mo, T. Jiang, J. Di, W. Tai, Z. Gu, *Chem. Soc. Rev.* **2014**, *43*, 3595.
[8] N. A. Bakh, A. B. Cortinas, M. A. Weiss, R. S. Langer, D. G. Anderson, Z. Gu, S. Dutta, M. S. Strano, *Nat. Chem.* **2017**, *9*, 937 – 943.
[9] O. Veiseh, B. C. Tang, K. A. Whitehead, D. G. Anderson, R. Langer, *Nat. Rev. Drug Discovery* **2015**, *14*, 45 – 57.
[10] J. Yu, Y. Zhang, H. Bomba, Z. Gu, *Bioeng. Transl. Med.* **2016**, *1*, 323 – 337.
[11] D. R. Owens, B. Zinman, G. B. Bolli, *Lancet* **2001**, *358*, 739 – 746.
[12] S. Wild, G. Roglic, A. Green, R. Sicree, H. King, *Diabetes Care* **2004**, *27*, 1047 – 1053.
[13] X. Jin, D. D. Zhu, B. Z. Chen, M. Ashfaq, X. D. Guo, *Adv. Drug Delivery Rev.* **2018**, *127*, 119 – 137.
[14] N. Jeandidier, S. Boivin, *Adv. Drug Delivery Rev.* **1999**, *35*, 179 – 198.
[15] S. Yaturu, *World J. Diabetes* **2013**, *4*, 1.
[16] R. B. Shah, M. Patel, D. M. Maahs, V. N. Shah, *Int. J. Pharm. Investig.* **2016**, *6*, 1.
[17] Y. Ohkubo, H. Kishikawa, E. Araki, T. Miyata, S. Isami, S. Motoyoshi, Y. Kojima, N. Furuyoshi, M. Shichiri, *Diabetes Res. Clin. Pract.* **1995**, *28*, 103 – 117.
[18] K. M. Bratlie, R. L. York, M. A. Invernale, R. Langer, D. G. Anderson, *Adv. Healthcare Mater.* **2012**, *1*, 267 – 284.
[19] D. R. Owens, *Nat. Rev. Drug Discovery* **2002**, *1*, 529 – 540.
[20] T. G. Farmer, T. F. Edgar, N. A. Peppas, *J. Pharm. Pharmacol.* **2008**, *60*, 1 – 13.
[21] V. Ravaine, C. Ancla, B. Catargi, *J. Controlled Release* **2008**, *132*, 2 – 11.
[22] Q. Wu, L. Wang, H. Yu, J. Wang, Z. Chen, *Chem. Rev.* **2011**, *111*, 7855 – 7875.
[23] J. Xie, A. Li, J. Li, *Macromol. Rapid Commun.* **2017**, *38*, 1700413.
[24] L. Zhao, L. Wang, Y. Zhang, S. Xiao, F. Bi, J. Zhao, G. Gai, J. Ding, *Polymers* **2017**, *9*, 255.
[25] S. B. Bankar, M. V. Bule, R. S. Singhal, L. Ananthanarayan, *Biotechnol. Adv.* **2009**, *27*, 489 – 501.
[26] M. J. Webber, D. G. Anderson, *J. Drug Targeting* **2015**, *23*, 651 – 655.
[27] M. L. Cortez, A. Lorenzo, W. A. Marmisollé, C. Von Bilderling, E. Maza, L. Pietrasanta, F. Battaglini, M. Ceolín, O. Azzaroni, *Soft Matter* **2018**, *14*, 1939 – 1952.
[28] Z. Gu, T. T. Dang, M. Ma, B. C. Tang, H. Cheng, S. Jiang, Y. Dong, Y. Zhang, D. G. Anderson, *ACS Nano* **2013**, *7*, 6758 – 6766.
[29] X. Chen, W. Wu, Z. Guo, J. Xin, J. Li, *Biomaterials* **2011**, *32*, 1759 – 1766.
[30] Z. W. Lim, Y. Ping, A. Miserez, *Bioconjugate Chem.* **2018**, *29*, 2176 – 2180.
[31] L. Zhao, C. Xiao, L. Wang, G. Gai, J. Ding, *Chem. Commun.* **2016**, *52*, 7633 – 7652.
[32] K. Ariga, Q. Ji, T. Mori, M. Naito, Y. Yamauchi, H. Abe, J. P. Hill, *Chem. Soc. Rev.* **2013**, *42*, 6322.
[33] J. Shi, Z. Jiang, *J. Mater. Chem. B* **2014**, *2*, 4435.
[34] D. M. Eckmann, R. J. Composto, A. Tsourkas, V. R. Muzykantov, *J. Mater. Chem. B* **2014**, *2*, 8085 – 8097.
[35] Z. Zeng, Y. She, Z. Peng, J. Wei, X. He, *RSC Adv.* **2016**, *6*, 8032 – 8042.
[36] J. Mosquera, I. García, L. M. Liz-Marzán, *Acc. Chem. Res.* **2018**, *51*, 2305 – 2313.
[37] W. Tai, R. Mo, J. Di, V. Subramanian, X. Gu, J. B. Buse, Z. Gu, *Biomacromolecules* **2014**, *15*, 3495 – 3502.
[38] J. Yu, C. Qian, Y. Zhang, Z. Cui, Y. Zhu, Q. Shen, F. S. Ligler, J. B. Buse, Z. Gu, *Nano Lett.* **2017**, *17*, 733 – 739.
[39] X. Hu, J. Yu, C. Qian, Y. Lu, A. R. Kahkoska, Z. Xie, X. Jing, J. B. Buse, Z. Gu, *ACS Nano* **2017**, *11*, 613 – 620.
[40] Y. Zhang, J. Wang, J. Yu, D. Wen, A. R. Kahkoska, Y. Lu, X. Zhang, J. B. Buse, Z. Gu, *Small* **2018**, *14*, 1704181.
[41] Z. Tong, J. Zhou, J. Zhong, Q. Tang, Z. Lei, H. Luo, P. Ma, X. Liu, *ACS Appl. Mater. Interfaces* **2018**, *10*, 20014 – 20024.
[42] C. Li, X. Liu, Y. Liu, F. Huang, G. Wu, Y. Liu, Z. Zhang, Y. Ding, J. Lv, R. Ma, Y. An, L. Shi, *Nanoscale* **2019**, *11*, 9163 – 9175.
[43] H. G. Bagaria, M. S. Wong, *J. Mater. Chem.* **2011**, *21*, 9454 – 9466.
[44] Y. Lapitsky, *Curr. Opin. Colloid Interface Sci.* **2014**, *19*, 122 – 130.
[45] V. S. Murthy, R. K. Rana, M. S. Wong, *J. Phys. Chem. B* **2006**, *110*, 25619 – 25627.
[46] R. K. Rana, V. S. Murthy, J. Yu, M. S. Wong, *Adv. Mater.* **2005**, *17*, 1145 – 1150.
[47] B. Hu, C. Pan, Y. Sun, Z. Hou, H. Ye, B. Hu, X. Zeng, *J. Agric. Food Chem.* **2008**, *56*, 7451 – 7458.
[48] S. E. Plush, M. Woods, Y.-F. Zhou, S. B. Kadali, M. S. Wong, A. D. Sherry, *J. Am. Chem. Soc.* **2009**, *131*, 15918 – 15923.
[49] K.-I. Jang, H. G. Lee, *J. Agric. Food Chem.* **2008**, *56*, 1936 – 1941.

[50] N. Zhao, H. G. Bagaria, M. S. Wong, Y. Zu, *J. Nanobiotechnol.* **2011**, *9*, 2.
[51] A. Farashishiko, S. E. Plush, K. B. Maier, A. Dean Sherry, M. Woods, *Chem. Commun.* **2017**, *53*, 6355 – 6358.
[52] V. S. Murthy, M. S. Wong in *Biomolecular Catalysis*, ACS, Washington, **2008**, pp. 214 – 232.
[53] H. Zhang, S. Mardyani, W. C. W. Chan, E. Kumacheva, *Biomacromolecules* **2006**, *7*, 1568 – 1572.
[54] P. G. Lawrence, Y. Lapitsky, *Langmuir* **2015**, *31*, 1564 – 1574.
[55] W. A. Marmisollé, J. Irigoyen, D. Gregurec, S. Moya, O. Azzaroni, *Adv. Funct. Mater.* **2015**, *25*, 4144 – 4152.
[56] M. L. Agazzi, S. E. Herrera, M. L. Cortez, W. A. Marmisollé, C. von Bilderling, L. I. Pietrasanta, O. Azzaroni, *Soft Matter* **2019**, *15*, 1640 – 1650.
[57] K. Lutz, C. Gröger, M. Sumper, E. Brunner, *Phys. Chem. Chem. Phys.* **2005**, *7*, 2812 – 2815.
[58] L. D'Agostino, M. Di Pietro, A. Di Luccia, *FEBS J.* **2005**, *272*, 3777 – 3787.
[59] J. Yu, M. A. Yaseen, B. Anvari, M. S. Wong, *Chem. Mater.* **2007**, *19*, 1277 – 1284.
[60] J. Yu, D. Javier, M. A. Yaseen, N. Nitin, R. Richards-Kortum, B. Anvari, M. S. Wong, *J. Am. Chem. Soc.* **2010**, *132*, 1929 – 1938.
[61] M. Mouslmani, J. M. Rosenholm, N. Prabhakar, M. Peurla, E. Baydoun, D. Patra, *RSC Adv.* **2015**, *5*, 18740 – 18750.
[62] P. Andreozzi, E. Diamanti, K. R. Py-Daniel, P. R. Cáceres-Vélez, C. Martinelli, N. Politakos, A. Escobar, M. Muzi-Falconi, R. Azevedo, S. E. Moya, *ACS Appl. Mater. Interfaces* **2017**, *9*, 38242 – 38254.
[63] S. E. Herrera, M. L. Agazzi, M. L. Cortez, W. A. Marmisollé, M. Tagliazucchi, O. Azzaroni, *ChemPhysChem* **2019**, *20*, 1044 – 1053.
[64] S. E. Herrera, M. L. Agazzi, M. L. Cortez, W. A. Marmisollé, C. Bilderling, O. Azzaroni, *Macromol. Chem. Phys.* **2019**, 1900094.
[65] K. Yoshida, R. Hashide, T. Ishii, S. Takahashi, K. Sato, J. Anzai, *Colloids Surf. B* **2012**, *91*, 274 – 279.
[66] W. Qi, X. Yan, J. Fei, A. Wang, Y. Cui, J. Li, *Biomaterials* **2009**, *30*, 2799 – 2806.
[67] K. Garajová, M. Zimmermann, M. Petrenčáková, L. Dzurová, M. Nemergut, Ľ. Škultéty, G. Žoldák, E. Sedlák, *Biophys. Chem.* **2017**, *230*, 74 – 83.
[68] M. D. Gouda, S. A. Singh, A. G. A. Rao, M. S. Thakur, N. G. Karanth, *J. Biol. Chem.* **2003**, *278*, 24324 – 24333.
[69] S. Khatun Haq, M. Faiz Ahmad, R. Hasan Khan, *Biochem. Biophys. Res. Commun.* **2003**, *303*, 685 – 692.
[70] B. Sharma, S. Mandani, T. K. Sarma, *J. Mater. Chem. B* **2014**, *2*, 4072 – 4079.
[71] J. S. Graça, R. F. de Oliveira, M. L. de Moraes, M. Ferreira, *Bioelectrochemistry* **2014**, *96*, 37 – 42.
[72] P. G. Lawrence, P. S. Patil, N. D. Leipzig, Y. Lapitsky, *ACS Appl. Mater. Interfaces* **2016**, *8*, 4323 – 4335.
[73] C. J. Thompson, L. Tetley, W. P. Cheng, *Int. J. Pharm.* **2010**, *383*, 216 – 227.
[74] G. Laucirica, W. A. Marmisollé, O. Azzaroni, *Phys. Chem. Chem. Phys.* **2017**, *19*, 8612 – 8620.
[75] R. Wilson, A. P. F. Turner, *Biosens. Bioelectron.* **1992**, *7*, 165 – 185.
[76] M. A. VandenBerg, M. J. Webber, *Adv. Healthcare Mater.* **2019**, *8*, 1801466.
[77] A. Matsumoto, T. Ishii, J. Nishida, H. Matsumoto, K. Kataoka, Y. Miyahara, *Angew. Chem. Int. Ed.* **2012**, *51*, 2124 – 2128; *Angew. Chem.* **2012**, *124*, 2166 – 2170.

Manuscript received: November 7, 2019
Accepted manuscript online: December 30, 2019
Version of record online: February 3, 2020